Arabian Journal of Chemistry (2021) **14**, 103320

King Saud University

**Arabian Journal of Chemistry**

www.ksu.edu.sa
www.sciencedirect.com

ORIGINAL ARTICLE

# Impact of ethynylene linkers on the optical and electrochemical properties of benzothiadiazole based alternate conjugated polymers

**Ahmed G.S. Al-Azzawi [a,b], Shujahadeen B. Aziz [c,d,*], Ahmed Iraqi [a], Ary R. Murad [e], Rebar T. Abdulwahid [c,f], Saad M. Alshehri [g], Tansir Ahamad [g]**

[a] *Department of Chemistry, University of Sheffield, Sheffield S3 7HF, UK*
[b] *Department of Chemistry, College of Education for Pure Science, University of Mosul, Iraq*
[c] *Hameed Majid Advanced Polymeric Materials Research Lab., Department of Physics, College of Science, University of Sulaimani, Qlyasan Street, Sulaimani 46001, Iraq*
[d] *Department of Civil Engineering, College of Engineering, Komar University of Science and Technology, Sulaimani 46001, Iraq*
[e] *Department of Pharmaceutical Chemistry, College of Medical and Applied Sciences, Charmo University, Chamchamal, Sulaimani 46023, Iraq*
[f] *Department of Physics, College of Education, University of Sulaimani, Old Campus, Sulaimani 46001, Iraq*
[g] *Department of Chemistry, King Saud University, P.O. Box 2455, Riyadh 11451, Saudi Arabia*

Received 12 May 2021; accepted 8 July 2021
Available online 15 July 2021

**KEYWORDS**

Conjugated polymers;
Optoelectronic;
Optical properties;
Benzothiadiazole (BT);
XRD study;
Thermal properties

**Abstract** The effect of ethynylene spacers on the bandgap of alternating polymers, comprising 4, 7-linked benzothiadiazole units and 2,7-linked fluorene, 2,7-linked carbazole or 2,6-linked anthracene repeat units has been investigated. The three novel polymers **PFDEBT**, **PCDEBT** and **PPA-DEBT** were prepared via the Sonogashira coupling reaction. The optical, electrochemical and thermal properties of the resulting polymers were compared and analysed. All polymers displayed low solubility in common organic solvents and have moderate molecular weights. Optical studies revealed that all the new ethynylene based-polymers displayed large bandgaps in excess of 2.1 eV. Results highlighted that incorporation of acetylene units between the benzothiadiazole electron accepting units and the other electron donor units over polymer chains leads to wide bandgaps as a result of the electron accepting properties of the acetylene units. The HOMO levels of the resulting polymers are unaffected by the different donor moieties used. However, varying the electron donor units can perturb the electron accepting ability of the main chain of polymers in this

* Corresponding author at: Hameed Majid Advanced Polymeric Materials Research Lab., Department of Physics, College of Science, University of Sulaimani, Qlyasan Street, Sulaimani 46001, Iraq.
E-mail addresses: amsss82@uomosul.edu.iq (A.G.S. Al-Azzawi), shujahadeenaziz@gmail.com, amsss82@uomosul.edu.iq (S.B. Aziz).
Peer review under responsibility of King Saud University.

Production and hosting by Elsevier

https://doi.org/10.1016/j.arabjc.2021.103320

series and their LUMO levels. Anthracene-based polymer (**PPADEBT**) displayed the lowest LUMO level, while the fluorene-based polymer (**PFDEBT**) displayed the highest LUMO level. All polymers showed good stability to thermal degradation. The amorphous nature of these polymers was confirmed with powder X-ray diffraction studies.



## 1. Introduction

Solar cell technology is one of the potential methods to solve global energy needs. Progress in plastic electronics technology, such as organic semiconducting materials used in bulk heterojunction (BHJ) solar cells, would assist to reduce the cost of manufacture of such devices (Hsu et al., 2021; Get et al., 2020; Venkateswararao et al., 2018; Li et al., 2019). Over the past decades, solution processed BHJ polymer solar cells (PSCs) have received increasing attention in the research community in view of its potential advantages such as light weight, high flexibility, low manufacturing costs and ease of synthesis of the polymers (Chen et al., 2020; Arabpour Roghabadi et al., 2018).

Recently, significant progress has been achieved in PSC devices with efficiencies exceeding 16% reported (Chang et al., 2020). It is imperative for the conjugated polymers used in this area to absorb a broad part of the solar spectrum, in order to obtain high power conversion efficiencies (PCE). Consequently, a variety of conjugated polymers have been developed which have low energy bandgaps in order to efficiently harvest energy from sunlight (Du et al., 2013; Sardar et al., 2015). At the molecular level, the bandgap ($E_g$) and the HOMO and LUMO energy levels can be effectively tuned to achieve high performance in such organic polymer solar cells (OPSC) (Roncali, 1997; Yang et al., 2015). One of the effective approaches in designing conjugated polymers with suitable energy bandgaps is to prepare polymers with alternating electron-releasing units and electron-withdrawing units over the same conjugated polymeric chain (Du et al., 2013; Cheng et al., 2009). It is well established that benzothiadiazole (BT) is one of the most commonly used electron acceptor units for the construction of low bandgap polymers as a result of its strong electron withdrawing ability in D-A systems (Zhou et al., 2012). In previous reports, BT-based conjugated polymers have exhibited high PCEs in solar cells when fabricated with fullerene derivatives as acceptors in OPSC devices. A series of D-A polymers were explored with alternating 2,7-linked carbazole, 2,7-linked fluorene or 2,6-linked anthracene units flanked by thiophene as electron donor units and BT units as electron acceptors. These polymers displayed good efficiencies ranging from 3.3 to 6.2 % when used with fullerene derivatives in BHJ solar cells (Almeataq et al., 2013; Watters et al., 2013; Kuznetsov et al., 2015). Another study investigated the effect of incorporation an indoline organic dye as an interfacial modifier in OPSC device using a heptazole: $PC_{60}BM$ as BHJ device, this showed an enhanced overall PCE from 1.26% to 2.51%. The researchers found that heptazole polymer showed excellent charge mobility via compatibility its LUMO levels when fabricated with $PC_{60}BM$ in photovoltaic devices (Lim et al., 2016). Previous report investigated the effect of molecular weight of polymer on photovoltaic performance of device. One of the most effective approaches towards an increase of the PCE in BHJ solar cells is to optimise the molecular weight of donor segment in OPSC devices. The results revealed that the charge carrier mobility in OPSC based on high and low molecular weight polymer was similar. However, light intensity dependence of current–voltage characteristics of low molecular weight device displayed poor device performance as a result of strong bimolecular recombination in the low $M_n$ polymer which limited its $J_{sc}$ value. It was found that OPSC device based on high $M_n$ polymer processes lower bulk resistance that improved the performance of device due to supressing bimolecular recombination to reach the highest PCE of device. (Xianqiang et al., 2016).

Large twist angles between BT units and their adjacent units on the conjugated polymer, can lead to decreased packing and conjugation lengths in the resulting D-A systems. This effect remains a challenge to improve the efficiency of D-A conjugated polymers (Anant et al., 2008). In order to enhance the packing and rigidity of polymer chains, a linker is often employed between the electron donor and acceptor units along the conjugated polymer backbone. Previous reports have shown that the incorporation of an ethynylene unit (weak electron withdrawing unit) into the main chain of conjugated polymers generally enlarges their electronic bandgaps and lowers their HOMO energy levels (Liu et al., 2001; Zhang et al., 2009), Qin and his group (Qin et al., 2012) highlighted the impact of ethynylene linkages on the π-conjugated polymers made of 5,7-dithien-2-yl-thieno (Venkateswararao et al., 2018; Li et al., 2019) pyrazine and phenylene with the achieved bandgaps of 1.55 and 1.36 eV, respectively. Furthermore, the outcomes revealed the improved solar cell performance such as higher short circuit current and open circuit voltage with better device performance. Another study reported the introduction of ethynylene units in a thiophene-based polymer and found that ethynylene units lead to a polymer with a deeper HOMO level (~0.3 eV) but a slightly higher bandgap (~0.15 eV) than poly (3-hexylthiophene) (P3HT). The ethynylene-based polymer showed a higher $V_{oc}$ value than P3HT (1.01 V *vs.* 0.62 V) in BHJ devices, however, it had a lower PCE than P3HT (Cremer et al., 2006). This was explained by low charge mobility in devices as a result of a lower aggregation of polymer chains in blends with PCBM for the ethynylene-based polymer, even though it showed good aggregation of polymer chains in pristine films. Different studies reported the preparation of conjugated polymers via Sonogashira coupling reaction procedure, through which the bandgap of the host matrix were tuned through employing ethynylene spacer (Michinobu et al., 2008; Pu and Liu, 2010).

In this study, we present an investigation on the use of the ethynylene linker in polymers comprising alternating electron donor moieties such as carbazole, fluorene or anthracene units and alternating benzothiadiazole electron accepting units. The

role of the ethynylene linker on the physical properties of the resulting polymers including their energy bandgaps and energy levels will be discussed. In addition, this study highlights the possibility of tuning the optical and thermal properties of the prepared polymers in a way to best meet the requirements for the renewable energy device applications such as solar cell. The three new conjugated polymers have been synthesised using the Sonogashira coupling reaction. Their optical, electrochemical and thermal properties were investigated and compared to analogous polymers with thiophene linkers instead of ethynylene linkers.

### 1.1. Experimental

#### 1.1.1. Materials

9,9-Dioctyl-2,7-diethynylfluorene **(2)** (Liu et al., 2013), 2,7-dibromo-9-(heptadecan-9-yl)-*9H*-carbazole (Saeki et al., 2012) and 2,6-dibromo-9,10-bis(4-(dodecyloxy)phenyl)anthra cene (Almeataq et al., 2013), were prepared according to literature procedures. 4;7 -Dibromobenzo[c]-1,2,5-thiadiazole **(1)** was purchased from Sigma Aldrich and used as received. All chemicals and solvents, with the exception of those stated below, were of reagent grade quality, purchased commercially and used without further purification unless otherwise stated. Tetrahydrofuran (THF) was distilled and dried over sodium benzophenone under an inert nitrogen atmosphere. Toluene was dried and distilled over sodium under an inert atmosphere. Acetonitrile was dried and distilled over phosphorus pentoxide under an inert argon atmosphere, then stored over molecular sieves (3 Å).

#### 1.1.2. Measurements

$^{1}H$ and $^{13}C$ nuclear magnetic resonance (NMR) spectra were recorded using on Bruker Avance 400 (MHz) NMR spectrometer at ambient temperature using chloroform-d ($CDCl_3$) with tetramethylsilane (TMS) as an internal standard. The NMR shifts are described by using the following abbreviations: singlet (s), doublet (d), double doublet (dd), triplet (t), multiple (m) and broad (br). Moreover, coupling constants (*J*) are calculated in Hertz (Hz) and chemical shifts in part per million (ppm). CHN analyses were performed on the Perkin Elmer 2400 CHN Elemental Analyzer. In addition, the flask combustion method was used for the analysis of halides and sulfur. Mass spectra of monomers were recorded on a Perkin Elmer Turbomass Mass Spectrometer equipped with auto system XL GC. It has the ability to operate in both chemical ionization (CI) and electron ionization (EI) modes. GPC measurements were conducted on polymer solutions using chloroform or 1,2,4-trichlorobenzene (TCB) as eluents at a flow rate of 1 $cm^3$ $mintue^{-1}$. The system was calibrated against a series of narrow polystyrene standards (polymer laboratories) using a 1037 Differential Refractive Detector. UV–visible absorption spectra were performed using a Hitachi U-2010 Double Beam UV/Visible Spectrophotometer. Solution samples of polymers in $CHCl_3$ were measured by using rectangular quartz cuvettes (light path = 10 mm). Thin films of the polymers were prepared for UV–visible absorption spectra measurements by dip coating quartz plates into approximately 1 mg $cm^{-3}$ solutions in chloroform, then drying at room temperature. Measurements were performed under ordinary laboratory condition. The measurements of CV were obtained from a Princeton Applied Research Model 263A Potentiostat/Galvanostat. Measurements were carried out at room temperature using tetrabutylammonium perchlorate ($TBAClO_4$) solution in acetonitrile (0.1 mol $dm^{-3}$) as the electrolyte solution. A three-electrode system was used consisting of an Ag/Ag + reference electrode (silver wire in 0.01 mol $dm^{-3}$ silver nitrate solution in the electrolyte solution), a platinum working electrode (2 mm-diameter smooth platinum disc, area = $3.14 \times 10^{-2}$ $cm^2$), and a platinum counter electrode (platinum wire). Polymer thin films were formed by drop casting 1.0 $mm^3$ of polymer solutions in chloroform (HPLC grade) (1 mg $cm^{-3}$) onto the working electrode (Pt disk), then dried in air. Ferrocene was employed as a reference redox system according to IUPAC's recommendation. (Terao et al., 2013) Thermogravimetric analyses (TGAs) were recorded using a Perkin Elmer TGA-1 Thermogravimetric analyzer at a scan rate of 10 °C $min^{-1}$ under inert conditions. Powder X-ray diffraction profiles of polymers were obtained using a Bruker D8 advance diffractometer with a CuK-α radiation source (1.5418 Å, rated as 1.6 kW). The scanning angle was performed over the range (2–40°).

#### 1.1.3. Preparation of monomers and polymers

*1.1.3.1. 9,9-Dioctyl-2,7-[bis(2′-trimethysilyl) ethynyl)] fluorine*. A tow-neck 100 ml round bottom flask containing a solution of 2,7-dibromo-9,9-dioctylfluorene (S3) (1.10 g, 2.01 mmol) in dry toluene (20 ml) and diisopropylamine (6 ml, degassed) was stirred and placed under an inert atmosphere. Copper (II) iodide (CuI) (0.016 g, 5%) and bis(triphenylphosphine) palladium(II) dichloride Pd(PPh3)2Cl2 (0.052 g, 4%) were added to the solution reaction then the system was degassed. After stirring for 0.5 h, a solution of trimethylsilyl acetylene (0.43 g, 0.62 ml, 4.40 mmol, d = 0.6 95 g/ml) in disopropylamine (4.0 ml, degassed) was added via syringe to the suspension. Purging of the inert gas was continued during and after the addition. The mixture was degassed and then heated to reflux overnight to give a reddish-brown suspension. The reaction was monitored by spot TLC to verify the completion of the reaction. After cooling the mixture to room temperature, the solvent was removed in vacuo to produce a crude product. The material was purified via chromatography over silica gel using petroleum ether as eluent to give a pure product as white crystals (1.10 g, 1.88 mmol, 94 %). The purity of the product was confirmed by TLC (single spot Rf = 0.5) in petroleum ether. $^{1}H$ NMR (400 MHz, $CDCl_3$) (δ/ppm): 7.61 (d, $J$ = 8.0 Hz, 2H), 7.47 (dd, $J$ = 8.0 and $J$ = 2.0 Hz, 2H), 7.43 (s, 2H), 1.94 (m, 4H), 1.27–1.0 (m, 20H), 0.84 (t, $J$ = 7.0 Hz, 6H), 0.57–0.48 (br, 4H), 0.30 (s, 18H). $^{13}C$ NMR (400 MHz, CDCl3) (δ/ppm): 150.93, 140.85, 131.22, 126.21, 121.73, 119.83, 106.07, 94.25, 55.23, 40.34, 31.79, 29.89, 29.24, 23.59, 22.60, 14.10, −0.06. Mass (EI + ): ($m/z$) ($M^{\cdot+}$) 582, 583, 584. Elemental analysis calculated for $C_{39}H_{58}Si_2$: C, 80.34; H, 10.03 found; C, 79.83; H, 9.82.

*1.1.3.2. 9,9-Dioctyl −2,7-diethynylfluorene* ***(2)***. A solution of compound (4) (1.00 g, 1.71 mmol) in dry THF (15 ml) was stirred under degassed conditions. KOH aqueous solution (2.5 ml, 25% wt) in methanol (10 ml) was slowly added to the above reaction mixture under an inert atmosphere. The reaction was left at room temperature for 2 h. The mixture reaction

was extracted with DCM (3 × 200 ml), washed with brine (2 × 200 ml) and dried over (MgSO4). The solvent was evaporated in vacuo to obtain white-yellow crystals as pure product (0.72 g, 1.64 mmol, 96 %). The product gave a single spot on TLC (Rf = 0.36) in 100% hexane. $^{1}$H NMR (400 MHz, $CDCl_3$) (δ/ppm): 7.65 (d, *J* = 8.0 Hz, 2H) 7.50 (dd, J = 8.0 and *J* = 2.0 Hz, 2H), 7.48 (s, 2H), 3.17 (s, 2H), 1.97–1.93 (m, 4H), 1.27–1.05 (m, 20H), 0.84(t, *J* = 7.0, 6H), 0.60–0.53 (br, 4H).$^{13}$C NMR (400 MHz, CDCl3) (δ/ppm): 151.05, 141.01, 131.25, 126.55, 120.84, 119.98, 84.53, 55.22, 40.21, 31.77, 29.94, 29.20, 23.65, 22.59, 14.08. Mass (EI + ): (*m*/*z*) ($M^{\cdot+}$). 438, 439, 440. Elemental analysis calculated for $C_{33}H_{42}$; C, 90.35; H, 9.65, found; C, 89.23; H, 9.59.

*1.1.3.3. 9-(Heptadecan-9-yl)-2,7-bis((trimethylsilyl)ethynyl)-9H-carbazole*. To a mixture of2,7-dibromo-9-(heptadecan-9-yl)-*9H*-carbazole (0.5 g, 0.88 mmol), CuI (0.008 g, 0.042 mmol) and $Pd(PPh_3)_2Cl_2$ (0.031 g, 0.035 mmol) in dry toluene (10 ml), was added diisopropylamine (6 ml) and placed under an inert atmosphere. To this mixture was slowly added *via* syringe, a solution of trimethylsilyl acetylene (0.191 g, 0.27 ml, 1.95 mmol) in disopropylamine (4.0 ml, degassed). The mixture was then degassed again and heated to 70 °C overnight. The reaction was monitored by TLC to verify the completion of the reaction. Upon completion, the mixture was cooled to room temperature and the solvent removed *in vacuo* to afford the crude product. Purification by column chromatography on silica gel using petroleum ether as the eluent afforded the product as a yellow powder (0.49 g, 94.2%). The product gave a single spot on TLC (Rf = 0.40) in petroleum ether.$^{1}$H NMR (400 MHz, $CDCl_3$) (δ/ppm): 7.98 (br, 2H); 7.67 (s, 1H); 7.53 (s, 1H), 7.34 (br, 2H)., 4.51 (m, 1H); 2.31–2.20 (br, 2H), 1.98–1.87 (m, 2H); 1.30–1.08 (m, 20H); 1.04–0.93 (br, 4H); 0.85 (t, *J* = 7.0 Hz, 6H); 0.32 (s, 18H).$^{13}$C NMR (400 MHz, $CDCl_3$) (δ/ppm): 142.08, 138.64, 123.69, 123.18, 122.99, 122.25, 120.32, 120.09, 119.82, 115.04, 112.62, 106.63, 93.55, 56.85, 33.67, 31.72, 29.37, 29.30, 29.12, 26.84, 22.57, 14.03, −0.08.Mass (EI+): (*m*/*z*) ($M^{\cdot+}$). 597.4, 598.4, 599.4. Elemental analysis calculated for $C_{33}H_{43}NSi_2$, C, 78.32; H, 9.94; N, 2.34; found; C, 78.30; H, 10.14; N, 2.09.

*1.1.3.4. 2,7-Diethynyl-9-(heptadecan-9-yl)-9H-carbazole (**3**)*. An aqueous solution of KOH (2.5 ml, 25.0%) in methanol (4 ml) was added dropwise to a single neck 100 ml flask containing 9-(heptadecan-9-yl)-2,7-bis((trimethylsilyl)ethynyl)-*9H*-carbazole (0.44 g, 0.73 mmol) in THF (10 ml) under argon atmosphere. The reaction system was degassed and stirred at ambient temperature for 3 h. The progress of the reaction was monitored by TLC. Upon completion, the mixture was extracted with dichloromethane (3 × 200 ml). The organic extracts were washed with water (2 × 200 ml) then dried over $MgSO_4$. The solvent was removed *in vacuo* to yield pure product **3** as a yellow viscous oil (0.18 g, 92%). The product gave a single spot on TLC (Rf = 0.45) in petroleum ether.$^{1}$H NMR (400 MHz, $CDCl_3$) (δ/ppm): 8.02 (br, 2H); 7.74 (s, 1H); 7.58 (s, 1H), 7.38 (br, 2H)., 4.51 (m, 1H); 3.19 (s, 2H); 2.31–2.20 (m, 2H), 1.98–1.89 (m, 2H); 1.29–1.09 (m, 20H); 1.04–0.93 (br, 4H); 0.85 (t, *J* = 7.0 Hz, 6H).$^{13}$C NMR (400 MHz, $CDCl_3$) (δ/ppm): 142.31, 138.62, 123.88, 123.05, 122.98, 122.44, 120.59, 120.31, 119.93, 118.84, 115.46, 112.97, 85.07, 56.85, 33.63, 31.74, 29.32, 29.28, 29.13, 26.80, 22.60, 14.07.Mass (EI +): (*m*/*z*) ($M^{\cdot+}$)0.453.3, 455.3, 454.3.Elemental analysis calculated for $C_{33}H_{43}N$, C, 87.36; H, 9.55; N, 3.09; found; C, 87.31; H, 9.62.; N, 3.05.

*1.1.3.5. 2, 6- bis ((trimethylsilyl)ethynyl)-9,10-bis(4-(dodecyloxy)phenyl)-anthracene*. A round bottom flask was charged with 2,6-dibromo-9,10-bis(4-(dodecyloxy)phenyl)-anthracene (0.44 g, 0.513 mmol), CuI (0.005 g, 0.026 mmol) and Pd $(PPh_3)_2Cl_2$ (0.018 g, 0.02 mmol) in dry toluene (20 ml), followed by diisopropylamine (6 ml, degassed). The mixture was degassed and placed under an inert atmosphere. To this solution was added, trimethylsilyl acetylene (0.099 g, 0.14 ml, 1.0 mmol) in disopropylamine (4.0 ml, degassed). The system was degassed again and then refluxed at 70 °C for 48 h. The reaction was monitored by TLC to follow its progress. Upon completion, the solvent was removed from *in vacuo* to obtain the crude product. The product was purified via silica gel column chromatography using petroleum ether: toluene (80: 20%) as eluent to yield the pure product as a yellow solid (0.39 g, 95%). The product gave a single spot on TLC (Rf = 0.5) in petroleum ether: toluene (80: 20%).$^{1}$H NMR (400 MHz, $CDCl_3$) (δ/ppm): 7.89 (br, 2H), 7.64 (d, *J* = 9.0 Hz, 2H), 7.35 (d, *J* = 9.0 Hz, 4H), 7.31 (dd,*J* = 9.0 and *J* = 2.0 Hz, 2H), 7.16 (d, *J* = 9.0 Hz, 4H), 4.14 (t, *J* = 7.0 Hz, 4H), 1.92 (m, 4H); 1.62–1.25 (br, 36H); 0.91 (t, *J* = 7.0 Hz, 6H), 0.26 (s, 18H).$^{13}$C NMR (400 MHz, $CDCl_3$) (δ/ppm): 158.79, 137.01, 132.42, 131.13, 130.22, 129.96, 129.86, 127.69, 127.25, 119.84, 114.53, 105.85, 95.47, 88.94, 68.20, 31.95, 29.71, 29.66, 29.51, 92.45, 29.39, 26.20, 22.72, 14.15, −0.05.Mass (EI+): (*m*/*z*) ($M^{\cdot+}$) 890.8, 891.8, 892.8. Elemental analysis calculated for $C_{60}H_{82}O_2Si_2$, C, 80.84; H, 9.27, found; C, 77.15; H, 8.76%.

*1.1.3.6. 2,6-Diethynyl-9,10-bis(4-(dodecyloxy)phenyl)-anthracene (**4**)*. To a solution of 2,6-bis((trimethylsilyl)ethynyl)-9,10 -bis(4-(dodecyloxy)phenyl)-anthracene (0.34 g, 0.38 mmol) in dry THF (15 ml) under an inert atmosphere, was slowly added a solution of KOH (2.5 ml, 25.0% aqueous solution) in methanol (4 ml) under vigorous stirring. The resulting mixture was stirred at ambient temperature for 4 h. The mixture was then extracted with dichloromethane (3 × 200 ml), then the organic extracts were washed with water (2 × 200 ml) then dried over $MgSO_4$. The solvent was removed *in vacuo* to obtain the crude product. The material was purified via silica gel column chromatography using petroleum ether: toluene (80:20 %) as eluent to afford pure product **4**as yellow crystals (0.22 g, 85.2%). The product provided a single spot on TLC (Rf = 0.45) in petroleum ether: toluene (80: 20 %).$^{1}$H NMR (400 MHz, $CDCl_3$) (δ/ppm): 7.94 (s, 2H), 7.69 (d, *J* = 9.0 Hz, 2H), 7.36–7.32 (br, 6H), 7.15 (d, *J* = 9.0 Hz, 4H), 4.13 (t, *J* = 7.0 Hz, 4H), 3.13 (s, 2H), 1.91 (m, 4H); 1.62–1.25 (br, 36H); 0.91 (t, *J* = 7.0 Hz, 6H).$^{13}$C NMR (400 MHz, $CDCl_3$) (δ/ppm): 158.89, 137.18, 132.29, 131.85, 130.25, 129.95, 129.72, 127.50, 127.41, 118.84, 114.57, 84.43, 78.14, 68.18, 31.95, 29.72, 29.66, 29.50, 92.43, 29.39, 26.19, 22.72, 14.15.Mass (EI+): (*m*/*z*) ($M^{\cdot+}$) 746.4, 747.4, 748.4.Elemental analysis calculated for $C_{54}H_{66}O_2$, C, 86.81; H, 8.90, found; C, 85.81; H, 8.78%.

*1.1.3.7. Poly[2,7-diethynyl-9,9-dioctylfluorene-alt-4,7-benzo[c] (Hsu et al., 2021; Get et al., 2020; Chen et al., 2020) thiadiazole]* ***PFDEBT***. A mixture of 4,7-dibromobenzo[c]-1,2, 5-thiadiazole (**1**) (0.058 g, 0.20 mmol), 2,7-diethynyl-9,9-dioctylfluorene(**2**) (0.087 g, 0.20 mmol), $Pd(PPh_3)_2Cl_2$ (0.019 g,

0.027 mmol) and CuI (0.009 g, 0.046 mmol) were added to a flask containing anhydrous THF (2 ml), toluene (4 ml) and diisopropylamine (3 ml, degassed) under inert conditions. The solution was stirred at reflux temperature (75 °C) for 6 h. The reaction was stopped and the mixture allowed to cool to room temperature, then it was slowly added into degassed methanol (300 ml) before being stirred overnight to give a precipitate. The solid precipitate was collected through a membrane filter. Then it was cleaned using Soxhlet extraction with different organic solvents in the following order: methanol, acetone, hexane, toluene, chloroform and chlorobenzene. The toluene fraction was obtained and concentrated to 10 ml *in vacuo* then poured into degassed methanol (300 ml). The resulting solution was stirred overnight then the precipitate collected through membrane filtration to afford the final polymer as a dark orange solid. $^1$H NMR (400 MHz, $CDCl_3$) (δ/ppm): 7.89 (s, 2H), 7.80–7.66 (br, 4H), 7.59–7.54 (br, 2H), 2.13–1.97 (br, 4H), 1.28–1.03 (br, 20H), 0.87–0.80 (br, 6H), 0.70–0.58 (br, 4H). Toluene fraction (17.5% yield) GPC in TCB at 140 °C, $M_n$ = 11600, $M_w$ = 29300, PDI = 2.5. Elemental Analysis calculated for $C_{39}H_{43}N_3S$: C, 79.96; H, 7.40; N, 7.17; S, 5.47%. Found: C, 76.85; H, 8.52; N, 4.23; S, 3.02%.

*1.1.3.8. Poly[2,7-diethynyl-9-(heptadecan-9-yl)carbazole-alt-4,7-benzo[c] (Hsu et al., 2021; Get et al., 2020; Chen et al., 2020)thiadiazole]* ***PCDEBT***. 7-Dibromobenzo[c]-1,2,5-thiadiazole (**1**) (0.058 g, 0.20 mmol) and 2,7-diethynyl-9-(heptadecan-9-yl)-9*H*-carbazole (**3**) (0.090 g, 0.20 mmol) were added to a round bottom flask and placed under argon. Dry toluene (4 ml) and THF (2 ml), were added followed by diisopropylamine (3 ml, degassed) and the solution was degassed again. Then $Pd(PPh_3)_2Cl_2$ (0.019 g, 0.027 mmol) and CuI (0.009 g, 0.046 mmol, 23%) were added to the degassed solution and heated to 75 °C for 4 h. Upon completion, the reaction was cooled to room temperature; then the mixture was added drop wise into degassed methanol (300 ml) and stirred overnight to give a precipitate. The precipitate was collected through a membrane filter. Then it was cleaned using Soxhlet extraction with different organic solvents in the following order: methanol, acetone, hexane, toluene, chloroform and chlorobenzene. The toluene fraction was obtained and concentrated to 10 ml *in vacuo* then poured into degassed methanol (300 ml). The resulting mixture was stirred overnight and the polymer collected by filtration as an orange powder. $^1$H NMR (400 MHz, $CDCl_3$) (δ/ppm): 8.20–8.06 (br, 2H), 7.96–7.75 (br, 4H), 7.65–7.40 (br, 2H), 4.70–4.53 (br, 1H), 2.42–2.26 (br, 2H), 2.09–1.94 (br, 2H) 1.36–0.98 (br, 24H), 0.84 (t, $J$ = 7.0, 6H). Toluene fraction (8.5% yield) GPC in TCBat 140 °C $M_n$ = 25000, $M_w$ = 80400, PDI = 3.2. Elemental Analysis calculated for $C_{39}H_{43}N_3S$: C, 79.96; H, 7.40; N, 7.17; S, 5.47%. Found: C, 76.85; H, 8.52; N, 4.23; S, 3.02%.

*1.1.3.9. Poly[2,6-diethynyl-9,10-bis(4-(dodecyloxy)phenyl)-anthracene-alt-4,7-benzo[c] (Hsu et al., 2021; Get et al., 2020; Chen et al., 2020)thiadiazole]* ***PPADEBT***. A round bottom flask was charged with 4,7-dibromobenzo[c]-1,2,5-thiadiazole (**1**) (0.058 g, 0.20 mmol) and 2,6-diethynyl-9,10-bis(4-(dodecyloxy)phenyl) anthracene (**4**) (0182 g, 0.20 mmol) under argon. Dry toluene (4 ml) and THF (2 ml) were then added, followed by diisopropylamine (3 ml, degassed) and the resulting solution degassed. To this mixture, $Pd(PPh_3)_2Cl_2$ (0.019 g, 0.027 mmol) and CuI (0.009 g, 0.046 mmol) were added. After addition, the solution was stirred at reflux temperature (75 °C) for 3 h. The reaction was stopped then the mixture allowed to cool to room temperature, then it was slowly added into degassed methanol (300 ml) before being stirred overnight to give a precipitate. The precipitate was collected through a membrane filter. Then it was cleaned using Soxhlet extraction with different organic solvents in the following order: methanol, acetone, hexane, toluene, chloroform and chlorobenzene. The toluene fraction was obtained and concentrated to 10 ml *in vacuo* then poured into degassed methanol (300 ml). The resulting mixture was stirred overnight and the solid was collected by filtration through a membrane filter. The final polymer was obtained as a dark red powder after drying in 21.0 % yield. $^1$H NMR (400 MHz, $CDCl_3$) (δ/ppm): 8.14–7.96 (br, 2H), 7.85–7.34 (br, 10*H*), 7.20 (t, $J$ = 8.0, 4H), 4.20–4.10 (br, 4H), 1.97–1.87 (br, 4H) 1.50–1.19 (br, 36H), 0.93–0.86 (br, 6H). Toluene fraction GPC in TCB at 140 °C, $M_n$ = 8700, $M_w$ = 21800, PDI = 2.5.Elemental Analysis calculated for $C_{60}H_{66}N_2O_2S$: C, 81.96; H, 7.57; N, 3.19; S, 3.657%. Found: C, 70.80; H, 7.22; N, 2.14; S, 2.17%.

## 2. Result and discussion

### 2.1. Synthesis and characterisation

The synthetic route for the preparation of the three conjugated polymers is outlined in Scheme 1. 4,7-Dibromobenzo[c]-1,2,5-thiadiazole (BT) (**1**) was reacted with respectively **2**, **3** and **4** in Sonogashira coupling reactions to produce polymers **PFDEBT** (yield = 17.5%), **PCDEBT** (yield = 8.5%) and **PPADEBT** (yield = 21%). The polymerisations were carried out using $Pd(PPh_3)_2Cl_2$ as the catalyst and CuI as co-catalyst along with diisopropylamine as the base in a mixture of anhydrous THF/-toluene solvent under inert atmosphere. All polymerisations were conducted until precipitates of the polymers were observed. The time of polymerisation reactions varied between 3 and 12 h. The obtained crude products formed were separated by precipitation in methanol then cleaned and fractionated with different organic solvents using Soxhlet extractions in order to remove catalyst impurities, unreacted monomers and low molecular weight oligomers. It was observed that the polymers displayed limited solubilities in the Soxhlet thimbles with different organic solvents such as methanol, acetone, hexane, toluene, chloroform and chlorobenzene at high temperatures during the extraction process, only their toluene fractions were separated and used for further analysis with large fractions of the products remaining behind in the thimbles of Soxhlet apparatus. This explains the low yields observed from these polymerisations. The products obtained from the Soxhlet (toluene fractions after drying) were soluble in common organic solvents such as chloroform, dichloromethane and dichlorobenzene due to low molecular weights of polymers which were obtained from Soxhlet. So only toluene fractions of these polymers can be separated and characterised which probably reflect the main properties of ethynylene-based polymers. The chemical structures of these polymers were confirmed by $^1$H NMR and elemental analysis. Details of the synthesis of the polymers and their characterisation are given in the experimental section.

Gel permeation chromatography (GPC) data of all polymers is summarised in Table 1 with their number–average

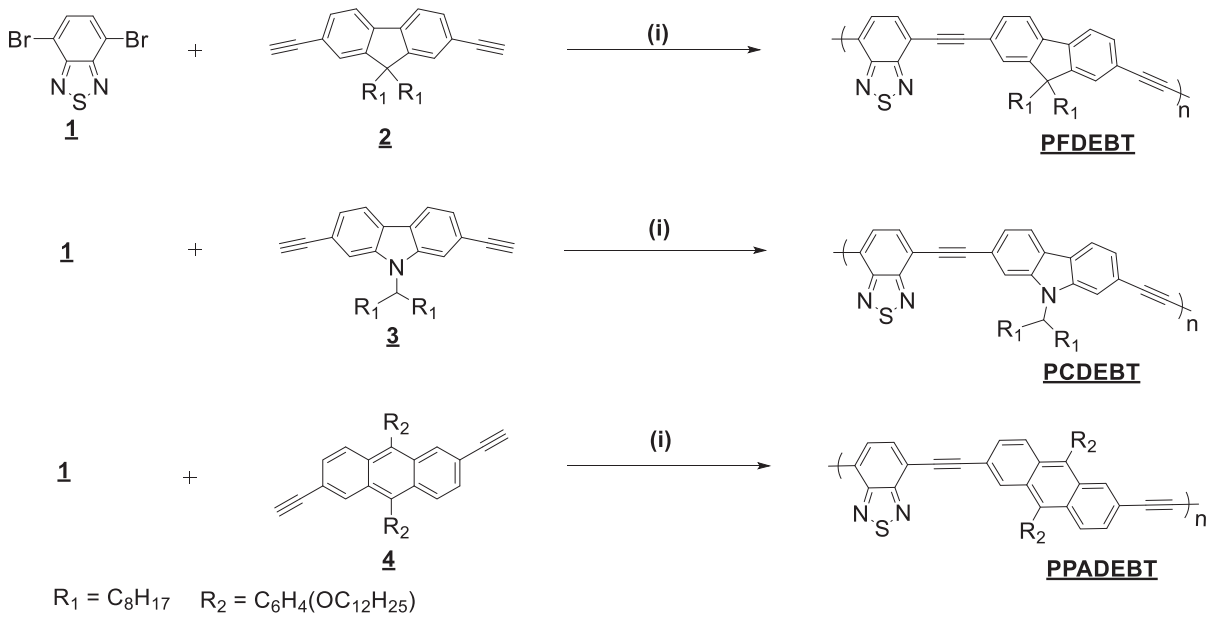


**Scheme 1** The synthetic route toward polymers **PFDEBT**, **PCDEBT** and **PPADEBT**.

**Table 1** GPC data of **PFDEBT**, **PCDEBT** and **PPADEBT**.

| Polymer [a] | Yield % | $M_n$ (Da) | $M_w$(Da) | PDI |
|---|---|---|---|---|
| **PFDEBT** | 17.5 | 11,600 | 29,300 | 2.5 |
| **PCDEBT** | 8.5 | 25,000 | 80,400 | 3.2 |
| **PPADEBT** | 21.0 | 8700 | 21,800 | 2.5 |

[a] Measurements conducted on toluene fractions of the polymers.

molecular weights ($M_n$), weight–average molecular weights ($M_w$) and polydispersity indexes. Measurements were conducted against polystyrene standards using 1,2,4-trichlorobenzene (TCB) as the eluent at 140 °C. These ethynylene-based polymers were separated in low yields (8.5 – 21%) from their toluene fractions. These fractions are the portions of polymers that are soluble but at the limit of their processability. Incorporation of ethynylene units along the polymer chains results in their aggregation as a consequence of much planar polymer conformations. (Terao et al., 2013) This leads to polymers to display poor solubility in Soxhlet thimble with other organic solvents at high temperature which extracted only low molecular weights of polymers from Soxhlet thimble (toluene fractions) and could not dissolve any of the left over polymers inside the thimble. The number average molecular weight $M_n$ of the anthracene-based polymer **PPADEBT** was estimated to be 8700 Da with a polydispersity of 2.5. These values are lower compared to those of the fluorene or carbazole-based polymers (**PFDEBT** and **PCDEBT**) respectively owing to the effect of a more extended conjugation and also the planarity of the anthracene repeat units. **PFEBTs** has been synthesised by Kan and Liu via Sonogashira coupling reaction, the ethynylene-based polymer exhibited remarkable aggregation and charge transfer character. (Pu and Liu, 2010) **PFDEBT** display similar aggregation attitude relative to its counterpart (**PFEBTs**) due to planarity of polymer chains.

### 2.2. Optical properties

The optical properties of all polymers were measured by UV–vis absorption spectroscopy in dilute chloroform solutions and in thin solid films (drop cast from chloroform solution). The optical spectra are shown in Fig. 1. All the optical data of the polymers are summarised in Table 2.

All polymers revealed absorption bands in chloroform solutions, in the range of 300–450 nm and 450–600 nm. The shorter wavelength absorption bands can be attributed to π-π* transitions, whereas the longer wavelength bands can be ascribed to the intramolecular charge transfer (ICT) bands between donor and acceptor moieties along the D-A polymer backbones. The thin films displayed red-shifted absorption bands relative to those observed in solutions. This phenomenon is caused by stronger π-π interactions and increased polymer chain aggregation in the solid state which increases their planarity. Interestingly, the small bathochromic shift (~20 nm) from dilute solution to solid state indicates that these polymers adopt relatively similar conformations whether in solutions or as films. Polymer **PPADEBT** displays an absorption maximum at 479 nm in solution and at 501 nm in films in addition to a

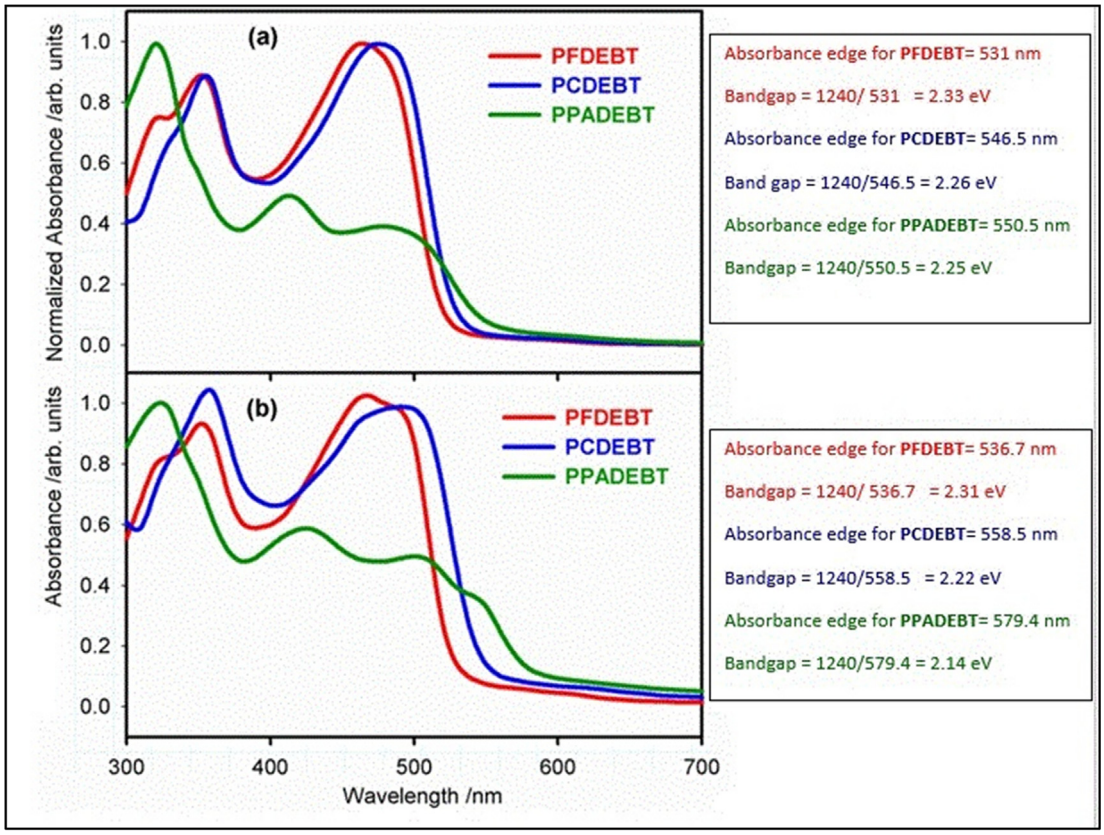


**Fig. 1** (a) Normalized absorption spectra of polymers in chloroform solution, (b) Absorption spectra of polymers as thin films.

**Table 2** Optical and electrochemical data for **PFDEBT**, **PCDEBT** and **PPADEBT.**

| Polymer | $\lambda_{max}$ solution (nm) | $\lambda_{max}$ film (nm) | $\lambda_{max}$ shoulder peak in film (nm) | ε [a] ($M^{-1}$ $cm^{-1}$) | $E_{g\ opt}$ [b] (eV) | $E^{Ox\ onset}$ [c] (V) | HOMO [d] (eV) | $E^{Red\ onset}$ [e] (V) | LUMO [f] (eV) | $E_{g\ elec}$ [g] (eV) |
|---|---|---|---|---|---|---|---|---|---|---|
| **PFDEBT** | 356–466 | 345–481 | – | 28,260 | 2.31 | 1.0 | −5.72 | −1.51 | −3.21 | 2.51 |
| **PCDEBT** | 358–479 | 361–492 | – | 31,183 | 2.22 | 0.94 | −5.66 | −1.41 | −3.31 | 2.35 |
| **PPADEBT** | 327–479 | 328–501 | 543 | 15,708 | 2.14 | 0.96 | −5.68 | −1.38 | −3.34 | 2.34 |

[a] Absorption coefficient measured (ε) at $\lambda_{max}$ = 466 nm for **PFDEBT**,479 nm for **PCDEBT,** and 479 nm for **PPADEBT** in chloroform solutions.
[b] Optical energy bandgap determined from the onset of absorption band in thin film.
[c] $E^{Ox\ onset\ t}$ is the onset oxidation potential determined by CV.
[d] HOMO position (*vs.* vacuum) determined from the onset of oxidation.
[e] $E^{Red\ onset}$ is the onset reduction potential determined by CV.
[f] LUMO position (*vs.* vacuum) determined from the onset of reduction.
[g] Electrochemical bandgap. HOMO and LUMO levels were determined, with respect of to ferrocene (as internal standard = − 4.8 eV below the vacuum level), via empirical relations: HOMO = -[($E^{Ox}$-0.08) + 4.8] eV, LUMO = -[($E^{Red}$-0.08) + 4.8] eV.

shoulder absorption at 543 nm. The shoulder absorption is related to arise from a pronounced stacking and aggregation of polymer chains in films formed by the anthracene-based polymer (Murad et al., 2021). The optical bandgaps, as determined from the onset of absorption in films, are 2.31, 2.22 and 2.14 eV for **PFDEBT**, **PCDEBT** and **PPADEBT** respectively. In comparison, the values of the absorption maxima of **PPADEBT** especially in thin films are red-shifted compared to those of **PFDEBT** and **PCDEBT**. The lower bandgap of **PPADEBT** in comparison to those of **PFDEBT** and **PCDEBT** is probably due to its ability to adopt more planar conformations in films and a more extended electronic delocalisation. The wider bandgap of the fluorene-based polymer **PFDEBT** in comparison to the carbazole-based polymer **PCDEBT** is attributed to the more electron donating nature of carbazole units in comparison to fluorene units; which leads to higher ICT along polymer chains of **PCDEBT** when compared to those of **PFDEBT**.

It is interesting to compare the optical properties of the present class of ethynylene-based polymers which incorporate

ethynylene units as linkers to those of analogous polymers which incorporate thiophene linkers. This will help to ascertain the effect of ethynylene units on the properties of these polymers. Polymers which have thiophene linkers rather than ethynylene linkers such as **PFDTBT**, **PCDTBT** and **PPADTBT** have been described in the literature (Almeataq et al., 2013; Alghamdi et al., 2013; Yi et al., 2011). These polymers exhibit remarkable hypochromic shifts in comparison with the ethynylene-based polymers. As an example, ethynylene-based polymer, **PFDEBT** displays a significant blue shift at $\lambda_{max}$ = 481 nm in films while its thiophene counterpart, **PFDTBT** has a $\lambda_{max}$ = 592 nm in drop cast films. Consequently, the optical bandgap of 2.31 eV for **PFDEBT** is wider than that of its thiophene analogue (1.86 eV). The same pattern is observed with **PCDEBT** and **PPADEBT** in comparison with their thiophene equivalent polymers. We attribute the blue shift in the absorption of the resulting polymers in this series of polymers is due to employing the acetylene linkers in alternating D-A polymers, which adopt more favoured and planar structures upon strong π-π interchain interactions (Terao et al., 2013). However, the planarity of these polymers decreased the molecular weights and solubilities of the polymers synthesised. In addition, the optical bandgaps were relatively large as a result of incorporating ethynylene spacers as weak electron-withdrawing units. These results indicate that the acetylene π-spacers between alternating units have a profound effect on the backbone of conjugated polymers and their properties. The ethynylene unit has slightly π-accepting properties as a result of the *sp* hybridization of its carbon centres which reduce the overall ICT between the strong π-accepting benzothiadiazole repeat units and the arylene units flanked by the ethynylene spacers along the polymer chains in these polymers. The synthesis of alternating copolymer based on 3,6-carbazoles as electron donor units with benzothiadiazole (BT) as electron acceptor units using ethynylene spacers has been reported (Michinobu et al., 2008). In comparison with **2, 7- PCDEBT** and its counterpart, the change of ethylene positions between carbazole donor and BT acceptors over the polymer chains did not show main differences in the optical properties of these polymers. The absorption maxima of **2, 7- PCDEBT** in $CHCl_3$ solution exhibits little red-shifted compared to **3, 6- PCDEBT** in $CH_2Cl_2$. This is probably due to solvatochromic effect. Consequently, the optical bandgap of 2.26 eV for **2, 7- PCDEBT** is smaller than that of its analogue (2.30 eV).

### 2.3. Electrochemical properties

Cyclic voltammetry (CV) studies were used to investigate the electrochemical properties of the polymers. The CV measurements were conducted on the polymers using drop-cast films in acetonitrile with tetrabutylammonium perchlorate as the electrolyte at scan rate of 100 mV/s under inert conditions. The cyclic voltammograms are shown in Fig. 2 and the HOMO and LUMO energy levels (*vs vacuum*) of the polymers as calculated from their first onsets of oxidation or reduction waves are summarised in Table 2. **PPADEBT** displayed a HOMO energy level of −5.68 eV which is comparable in value to that of **PCDEBT**, suggesting comparable electron donating ability of the 2,6-linked anthracene units and the 2,7-linked carbazole repeat units. **PFDEBT** displays a slightly lower lying

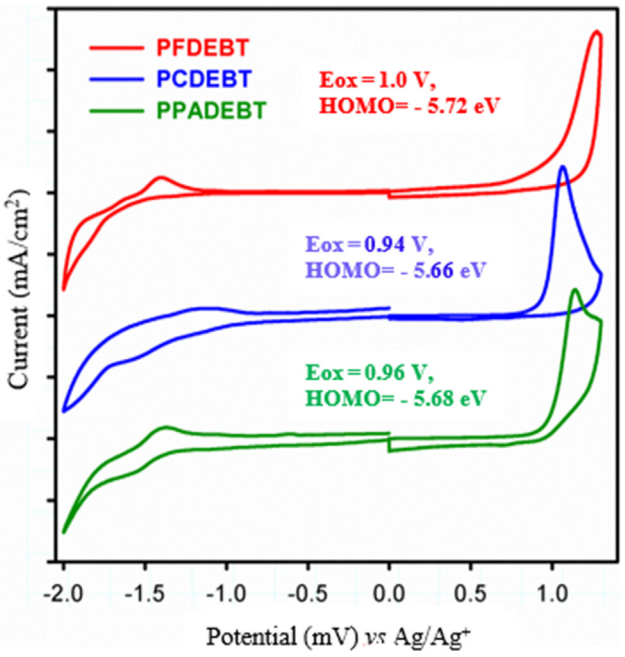


**Fig. 2** Cyclic voltammograms of the polymer films.

HOMO energy level relative to the other two polymers at −5.72 eV due to the reduced electron donating properties of the fluorene repeat units. However, the variation in the position of the HOMO levels of this series of polymers is not majorly affected by the nature of their electron donating moieties. It can be seen from Table 2 that the change of donor moieties affects the LUMO energy levels of the polymers to a greater extent. Incorporation of acetylene units between the BT units and the other electron donor units over polymer chains reduce the donating ability of donor moieties over polymeric chains as a result of the slight electron accepting properties of the acetylene units therefore the HOMO levels of the resulting polymers are unaffected by the different donor moieties. The LUMO level of **PFDEBT** (-3.21 eV) is about 0.1 eV closer to the vacuum level than the other two polymers in this series of polymers, **PCDEBT** and **PPADEBT** which display similar LUMO levels at −3.31 and −3.34 eV respectively. These results indicate that varying the electron donor units in these polymers perturb more the electron accepting ability of the main chain of polymers in these materials.

A comparison of the electrochemical properties of the resulting polymers, **PFDEBT**, **PCDEBT** and **PPADEBT** with their thiophene analogues reveals considerable lowering of the HOMO energy levels for the ethynylene-based polymers, resulting in wider bandgap polymers when compared to their thiophene counterparts. Indeed a series of thiophene analogues, **PFDTBT**, **PCDTBT** and **PPADTBT** reported in the literature (Almeataq et al., 2013; Alghamdi et al., 2013; Yi et al., 2011), display deeper HOMO energy levels and smaller bandgap polymers relative to the new synthesised ethynylene polymers in this series. Incorporation of ethynylene units as weak electron-withdrawing units in the main chain of conjugated polymers instead of the electron donating thiophene units is responsible for lowering the HOMO energy levels of the resulting polymers upon decreasing the electron donating ability of the donor segments on the polymer chains (Li

et al., 2011), resulting in an enlarged bandgap. As an example, the HOMO level of the ethynylene polymer **PFDEBT** is −5.72 eV while the HOMO level of its thiophene analogue **PFDTBT** at −5.34 eV. A similar comparison indicates that the HOMO level of **PPADEBT** is at −5.68 eV while that of its corresponding thiophene analogue **PPADTBT** has a HOMO level at −5.44 eV. These findings indicate how the ethynylene units could increase the planarity of polymer chains while at the same time changing the electronic properties of the resulting polymers and increasing their energy bandgaps. Comparison of the electrochemical properties of polymers without acetylene units with those that have acetylene units should ascertain the effects of incorporating acetylene linkers over the main chains of the polymers. The is properties of ethynylene-based polymer (**PCDEBT**) displayed better electrochemical properties compared to its analogue without ethynylene spacers which was synthesised by Squeo and co-workers (Squeo et al., 2019), this comparison indicated that **PCDEBT** has shallower lying HOMO energy levels (−5.66 eV) relative to its counterpart at − 5.80. The LUMO level of **PCDEBT** counterpart (−3.01 eV) is about 0.3 eV closer to the vacuum level than the ethylene-based polymers at – 3.31 eV although these polymers possess same donor (carbazole) and acceptor (BT) units except linker units. The introduction of ethynylene units over the main polymeric chains results in lower bandgap compared to its counterpart due to adopt of more planar structures which improves the interaction packing of the polymer.

### *2.4. Thermal properties and XRD studies*

Thermogravimetric analysis (TGA) studies were performed on the polymers under a nitrogen atmosphere at a heating rate of 10 °C/min. The TGA plots (Fig. 3) suggest that these polymers possess good thermal stability with decomposition temperature ($T_d$) (5% weight loss) over 240 °C except **PFDEBT** which showed low thermal stability. The TGA curves reveal that the 5% weight loss temperature ($T_d$) for **PFDEBT**, **PCDEBT** and **PPADEBT** were found to be respectively at 240 °C, 249 °C and 330 °C. For all polymers, the first step in the degradation can be ascribed to loss of alkyl and alkoxy chains from the donor moieties of the polymers. Above 500 °C, degradation of the

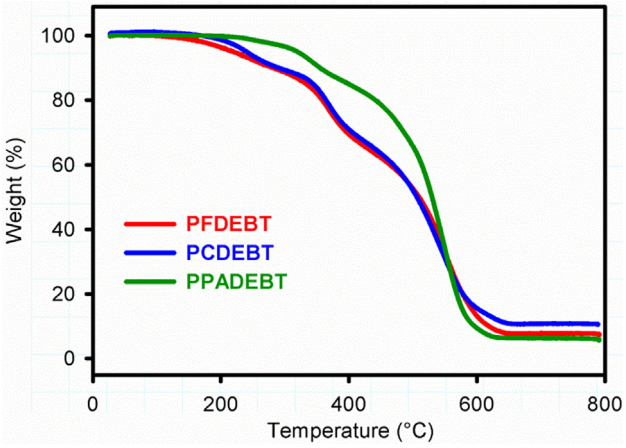


**Fig. 3** TGA plots of the resulting polymers with a heating rate of 10 °C/min under $N_2$.

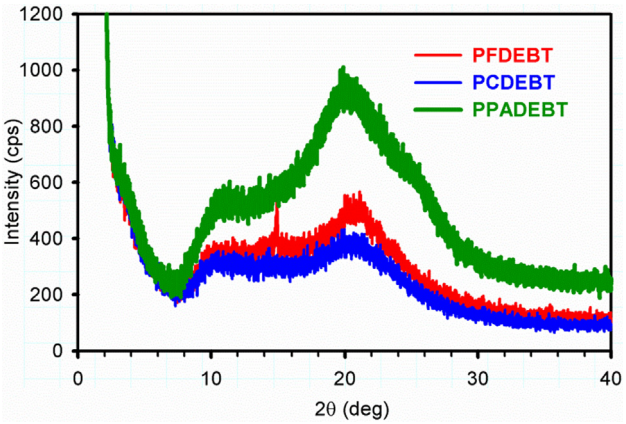


**Fig. 4** Powder XRD profiles of the target polymers.

polymer chains follows with a total weight loss of about 92%, 89% and 93% respectively for **PFDEBT**, **PCDEBT** and **PPADEBT** that is observed when the temperature is above 600 °C. The sufficient thermal stability of these polymers is related to the good thermal stability of BT units in the resulting polymers. For the purpose of comparison, **PPADEBT** exhibited a higher thermal stability with two step degradations, while **PFDEBT** and **PCDEBT** showed an apparent three step degradation process. The outcomes revealed that different thermal behaviours of these polymers come from varying electron donor moieties of these polymers. Generally, the thermal stabilities of these polymers are adequate for their applications in solar cells and other electronic devices.

Powder X-ray diffraction profiles of polymers **PFDEBT**, **PCDEBT** and **PPADEBT** were recorded (Fig. 4). A more pronounced diffraction peak appeared at 2$\theta$ value of 20.6° for **PPADEBT**, suggesting the polymer adopt a relatively more ordered structure in the solid state compared to the other two polymers. This corresponds to a π-π distance of 4.30 Å between polymer chains. **PFDEBT** and **PCDEBT** display weak and broad peaks in the wide-angle region at 2$\theta$ values of 20.7° and 20.8°, respectively. Clearly the low intensity of these diffraction peaks indicate that these two polymers adopt more amorphous structures with a distance of 4.29 and 4.27 Å between polymer chains for **PFDEBT**, **PCDEBT**, respectively. Interestingly, all polymers do not display any apparent peaks in the low-angle region. It can be seen that introduction of the anthracene-donor moiety in this series of polymers leads to more π-π stacking in the polymer backbones by increasing intermolecular interactions thus increasing the planarity of polymer chains and reducing the bandgap of polymers. Improved molecular packing of polymer chains is required for efficient charge carriers in BHJ devices. Thus, we believe that device fabricated from **PPADEBT** should provide improved charge carrier mobilities and $J_{sc}$ values; as a result of the enhanced π-π stacking of polymer chains.

## 3. Conclusion

In this study, a series of new D-A conjugated polymers **PFDEBT**, **PCDEBT** and **PPADEBT** containing acetylene π-spacers in the main backbone of conjugated polymers were synthesised based on 2,7-linked fluorene, 2,7-linked carbazole

or 2,6-linked anthracene repeat units as donor moieties and 2,1,3-benzothiadiazile (BT) alternate repeat units as acceptor moieties. The polymers were successfully prepared by the Sonogashira cross-coupling reactions. Moreover, their optical, electrochemical, thermal and structural properties were systematically investigated. The resulting polymers were obtained in low yields in view of their low solubilities. The introduction of ethynylene linkers over the main chains of polymers will adopt more planar conformations, resulting in the reduced solubilities and molecular weights of polymers. Compared with the thiophene-based polymers, the ethynylene-based polymers displayed more pronounced blue-shifted absorption spectra and larger bandgaps owing to the incorporation of acetylene units into the alternate D-A polymers. This phenomenon is arisen from the electronic effects, since the ethynylene units can be considered as weak electron acceptors. **PPADEBT** exhibits a lower bandgap relative to the other two ethynylene-based polymers. It also exhibits wider absorption bands and absorption shoulders than the other two polymers owing to its extended conjugated system. Incorporation of ethynylene linkers in this series of polymers leads to deep HOMO energy levels relative to other analogous donor–acceptor polymers. Further investigations into the use of this new class of polymers in BHJs are currently underway.

## Declaration of Competing Interest

The authors declare that they have no known competing financial interests or personal relationships that could have appeared to influence the work reported in this paper.

## Acknowledgements

We would like to acknowledge Iraqi-HCED and Mosul university-Iraq for financial support of this work. The authors (S. M. Alshehri, T. Ahmed) are grateful to the researchers supporting project number (RSP-2020/29), King Saud University, Saudi Arabia for funding.

## Appendix A. Supplementary material

Supplementary data to this article can be found online at https://doi.org/10.1016/j.arabjc.2021.103320.

## References

Alghamdi, A.A., Watters, D.C., Yi, H., Al-Faifi, S., Almeataq, M.S., Coles, D., Kingsley, J., Lidzey, D.G., Iraqi, A., 2013. Selenophene vs. thiophene in benzothiadiazole-based low energy gap donor–acceptor polymers for photovoltaic applications. J. Mater. Chem. A 1 (16), 5165–5171.

Almeataq, M.S., Yi, H., Al-Faifi, S., Alghamdi, A.A.B., Iraqi, A., Scarratt, N.W., Wang, T., Lidzey, D.G., 2013. Anthracene-based donor–acceptor low band gap polymers for application in solar cells. Roy. Soc. Chem. 49, 2252–2254.

Anant, P., Lucas, N.T., Jacob, J., 2008. A simple route toward the synthesis of bisbenzothiadiazole derivatives. Org. Lett. 10 (24), 5533–5536.

Chang, Y., Lau, Tsz-Ki, Chow, P.C.Y., Wu, N., Su, D., Zhang, W., Meng, H., Ma, C., Liu, T., Li, K., Zou, X., Wong, K.S., Lu, X., Yan, H., Zhan, C., 2020. A 16.4% efficiency organic photovoltaic cell enabled using two donor polymers with their side-chains oriented differently by a ternary strategy. J. Mater. Chem. A 8 (7), 3676–3685.

Chen, J., Chen, Y., Feng, Liang-Wen, Gu, C., Li, G., Su, N., Wang, G., Swick, S.M., Huang, W., Guo, X., Facchetti, A., Marks, T.J., 2020. Hole (donor) and electron (acceptor) transporting organic semiconductors for bulk-heterojunction solar cells. EnergyChem 2 (5).

Cheng, Y.-J., Yang, S.-H., Hsu, C.-S., 2009. Synthesis of conjugated polymers for organic solar cell applications. Chem. Rev. 109 (11), 5868–5923.

Chueh, C.C., Jen, A.K.Y., 2019. Recent advances in molecular design of functional conjugated polymers for high-performance polymer solar cells. Prog. Polym. Sci. 99.

Cremer, J., Bäuerle, P., Wienk, M.M., Janssen, R.A.J., 2006. High open-circuit voltage poly (ethynylene bithienylene): Fullerene solar cells. Chem. Mater. 18 (25), 5832–5834.

Du, C., Li, W., Li, C., 2013. Ethynylene-containing donor–acceptor alternating conjugated polymers: Synthesis and photovoltaic properties. J. Polym. Sci., Part A: Polym. Chem. 51 (2), 383–393.

Hsu, F.C., Lin, Y.A., Li, C.P., 2021. Stable polymer solar cells using conjugated polymer as solvent barrier for organic electron transport layer. Organic Electron. 89.

Islam, S.M., Singh, S., Mahala, P., 2020. Organic polymer bilayer structures for applications in flexible solar cell devices. Microelectron. Eng. 222.

Kuznetsov, I.E., Akkuratow, A.V., Susarova, D.K., Anokhin, D.V., Moskvin, Y.L., Kluyev, M.V., Peregudove, A.S., Troshin, P.A., 2015. Statistical carbazole–fluorene–TTBTBTT terpolymers as promising electron donor materials for organic solar cells. Chem. Commun. 51 (35), 7562–7564.

Li, J., Yan, M., Xie, Y., Qiao, Q., 2011. Linker effects on optoelectronic properties of alternate donor–acceptor conjugated polymers. Energy Environ. Sci. 4 (10), 4276–4283.

Lim, I., Bui, H.T., Shrestha, N.K., Lee, J.K., Han, S.-H., 2016. Interfacial engineering for enhanced light absorption and charge transfer of a solution-processed bulk heterojunction based on heptazole as a small molecule type of donor. ACS Appl. Mater. Interfaces 8 (13), 8637–8643.

Liu, B., Yu, W.-L., Pei, J., Liu, S.-Y., Lai, Y.-H., Huang, W., 2001. Design and synthesis of bipyridyl-containing conjugated polymers: effects of polymer rigidity on metal ion sensing. Macromolecules 34 (23), 7932–7940.

Liu, S., Zhang, K., Lu, J., Zhang, J., Yip, H.-L., Huang, F., Cao, Y., 2013. High-efficiency polymer solar cells via the incorporation of an amino-functionalized conjugated metallopolymer as a cathode interlayer. J. Am. Chem. Soc. 135 (41), 15326–15329.

Michinobu, T., Okoshi, K., Osako, H., Kumazawa, H., Shigehara, K., 2008. Band-gap tuning of carbazole-containing donor–acceptor type conjugated polymers by acceptor moieties and π-spacer groups. Polymer 49 (1), 192–199.

Murad, A.R., Iraqi, A., Aziz, S.B., Almeataq, M.S., Abdullah, S.N., Brza, M.A., 2021. Characteristics of low band gap copolymers containing anthracene-benzothiadiazole dicarboxylic imide: Synthesis, optical, electrochemical, thermal and structural studies. Polymers 13 (1), 62.

Pu, K.-Y., Liu, B., 2010. Fluorescence turn-on responses of anionic and cationic conjugated polymers toward proteins: effect of electrostatic and hydrophobic interactions. J. Phys. Chem. B 114 (9), 3077–3084.

Qin, H., Li, L., Li, Y., Peng, X., Peng, J., Cao, Y., Ismayil, N., Shi, W., 2012. Enhancing the performance of a thieno [3-4-b] pyrazine based polymer solar cell by introducing ethynylene linkages. Eur. Polym. J. 48 (12), 2076–2084.

Roghabadi, F.A., Ahamdi, N., Ahamdi, V., Carlo, A.D., Aghmiuni, K.O., Tehrani, A.S., Ghoreishi, F.S., Payandeh, M., Fumani, N.M. R., 2018. Bulk heterojunction polymer solar cell and perovskite solar cell: Concepts, materials, current status, and opto-electronic properties. Sol. Energy 173, 407–424.

Roncali, J., 1997. Synthetic principles for bandgap control in linear π-conjugated systems. Chem. Rev. 97 (1), 173–206.

Saeki, A., Yoshikawa, S., Tsuji, M., Koizumi, Y., Ide, M., Vijayakumar, C., Seki, S., 2012. A versatile approach to organic photovoltaics evaluation using white light pulse and microwave conductivity. J. Am. Chem. Soc. 134 (46), 19035–19042.

Sardar, S., Kar, P., Remita, H., Liu, B., Lemmens, P., Pal, S.K., Ghosh, S., 2015. Enhanced charge separation and FRET at heterojunctions between semiconductor nanoparticles and conducting polymer nanofibers for efficient solar light harvesting. Sci. Rep. 5.

Squeo, B.M., Carulli, F., Lassi, E., Galeotti, F., Giovanella, U., Luzzati, S., Pasini, M., 2019. Benzothiadiazole-based conjugated polyelectrolytes for interfacial engineering in optoelectronic devices. Pure Appl. Chem. 91 (3), 477–488.

Terao, J., Wadahama, A., Matono, A., Tada, T., Watanabe, S., Seki, S., Fujihara, T., Tsuji, Y., 2013. Design principle for increasing charge mobility of π-conjugated polymers using regularly localized molecular orbitals. Nat. Commun. 4 (1), 1–9.

Venkateswararao, A., Liu, S.W., Wong, K.T., 2018. Organic polymeric and small molecular electron acceptors for organic solar cells. Mater. Sci. Eng.: R: Rep. 124, 1.

Watters, D.C., Yi, H., Pearson, A.J., Kingsley, J., Iraqi, A., Lidzey, D. G., 2013. Fluorene-Based Co-polymer with High Hole Mobility and Device Performance in Bulk Heterojunction Organic Solar Cells. Macromol. Rapid Commun. 34 (14), 1157–1162.

Xianqiang, L., Jun, L., Hong, W., Dan, W., Xiaohong, T., 2016. The effects of molecular weight of a new hole transporting polymer on the organic solar cells performance. Procedia Eng. 139, 140–146.

Yang, Y.M., Chen, W., Dou, L., Chang, W.-H., Duan, H.-S., Bob, B., Li, G., 2015. High-performance multiple-donor bulk heterojunction solar cells. Nat. Photonics 9 (3), 190–198.

Yi, H., Al-Faifi, S., Iraqi, A., Watters, D.C., Kingsley, J., Lidzey, D. G., 2011. Carbazole and thienyl benzo [1, 2, 5] thiadiazole based polymers with improved open circuit voltages and processability for application in solar cells. J. Mater. Chem. 21 (35), 13649–13656.

Zhang, S., Fan, H., Liu, Y., Zhao, G., Li, Q., Li, Y., Zhan, X., 2009. Soluble dithienothiophene polymers: Effect of link pattern. J. Polym. Sci., Part A: Polym. Chem. 47 (11), 2843–2852.

Zhou, H., Yang, L., You, W., 2012. Rational design of high performance conjugated polymers for organic solar cells. Macromolecules 45 (2), 607–632.